AIP | Review of Scientific Instruments

Development of a high resolution and high dispersion Thomson parabola

D. Jung, R. Hörlein, D. Kiefer, S. Letzring, D. C. Gautier et al.

Citation: Rev. Sci. Instrum. **82**, 013306 (2011); doi: 10.1063/1.3523428
View online: http://dx.doi.org/10.1063/1.3523428
View Table of Contents: http://rsi.aip.org/resource/1/RSINAK/v82/i1
Published by the AIP Publishing LLC.

Development of a high resolution and high dispersion Thomson parabola

D. Jung,[1,2,3,a)] R. Hörlein,[2,3] D. Kiefer,[2,3] S. Letzring,[1] D. C. Gautier,[1] U. Schramm,[4] C. Hübsch,[2] R. Öhm,[2] B. J. Albright,[1] J. C. Fernandez,[1] D. Habs,[2,3] and B. M. Hegelich[1,2]
[1]*Los Alamos National Laboratory, Los Alamos, New Mexico 87545, USA*
[2]*Department für Physik, Ludwig-Maximilians-Universität München, D-85748 Garching, Germany*
[3]*Max-Planck-Institut für Quantenoptik, D-85748 Garching, Germany*
[4]*Forschungszentrum Dresden Rossendorf, D-01314 Dresden, Germany*

(Received 20 August 2010; accepted 10 November 2010; published online 31 January 2011)

Here, we report on the development of a novel high resolution and high dispersion Thomson parabola for simultaneously resolving protons and low-Z ions of more than 100 MeV/nucleon necessary to explore novel laser ion acceleration schemes. High electric and magnetic fields enable energy resolutions of $\Delta E/E < 5\%$ at 100 MeV/nucleon and impede premature merging of different ion species at low energies on the detector plane. First results from laser driven ion acceleration experiments performed at the Trident Laser Facility demonstrate high resolution and superior species and charge state separation of this novel Thomson parabola for ion energies of more than 30 MeV/nucleon. © *2011 American Institute of Physics*. [doi:10.1063/1.3523428]

I. INTRODUCTION

Laser ion acceleration has been of particular interest over the last decade in fundamental as well as applied sciences.[1–3] A wide variety of applications has been proposed utilizing laser accelerated ions such as ion cancer therapy,[4] proton radiography,[5] and ion-driven fast ignition.[6,7] Most applications require very high ion energies, such as 0.5 GeV carbon ions for fast ignition or >200 MeV protons and 2–4 GeV carbon ions for cancer therapy.[4] Conventional laser ion acceleration schemes such as target normal sheath acceleration (TNSA) (Ref. 8) have so far only yielded much lower particle energies which could be measured with relatively simple and compact particle spectrometers. In TNSA, an intense laser is focused on a several micron thick target, where electrons heated by the laser set up a virtual cathode on the backside of the target. In this field of several TV/m, predominantly protons are accelerated as they shield the field to heavier ions. Highest proton energies achieved by TNSA are about 60 MeV (Ref. 9) with typical energies of 20–30 MeV for large Nd:glass laser systems and only 5–10 MeV for Ti:sapphire systems. Acceleration of heavier ions was limited to a few MeV/nucleon[10] using TNSA, due to the lower charge to mass ratio. Recently, numerous publications predict proton as well as ion acceleration to energies of several hundreds of MeV up to the GeV range by exploiting mechanisms such as radiation pressure acceleration (RPA) at lower intensities (10^{19}–10^{20} W/cm^2 using circular polarization)[11–13] and at higher intensities in the laser piston regime[14] or the breakout after burner (BOA). (Refs. 15 and 16) While in RPA, the light pressure continuously pushes electrons accelerating all ion species very efficiently,[17] and in BOA, strong volumetric heating[3] in a relativistically transparent target eventually leads to ion energies in the GeV range. To validate these simulations and measure those high ion energies, a new generation of ion spectrometers for use at ultrahigh intensity lasers needs to be developed which exhibits a high enough resolution in both particle energy and mass to charge state. Recent experiments already showed simultaneous acceleration of carbon C^{6+} ions and protons exceeding 40 MeV/nucleon (Ref. 18) in the BOA regime. At these energies, the merging of traces of different ion species is already a major issue in conventional ion spectrometers and exploiting these novel acceleration mechanisms has just started; a significant increase in energy of laser accelerated ions exceeding 100 MeV/nucleon is to be expected in the near future. The steady improvement of laser driven ion acceleration and the continuous increase of ion energies consequently demands novel high resolution ion diagnostics in order to properly resolve the ions in terms of their charge to mass ratio and their kinetic energy. The Thomson parabola (TP) (Ref. 19) concept is chosen due to the reliability of the static electric and magnetic fields as well as the inherent simplicity of the physics. Still, considerable effort is required in order to design a TP with sufficient energy resolution for simultaneous proton and ion detection in the >100 MeV/nucleon range, as premature merging of different ion species traces becomes a serious problem at such energies. In this paper, we report on the development of a such high resolution and high dispersion TP allowing for detection of proton and ion traces at energies exceeding 100 MeV/nucleon with an energy resolution $\Delta E/E < 5\%$ and a superior separation of different charge to mass ratios.

The report is structured as follows: in Sec. II, the principle theory of the TP and analysis of its resolution and charge to mass separation depending on the main TP parameters will be reviewed; Sec. III describes key aspects of the new high resolution TP and compares them with other TP parameters commonly used. Finally, first results from an experiment at the Trident laser facility[20,21] are presented demonstrating the superior resolution and extremely high trace separation of our novel TP using a beam of protons and C^{6+} ions from laser ion acceleration in the BOA regime exceeding 30 MeV/nucleon.

a)Electronic mail: daniel.jung@physik.uni-muenchen.de.

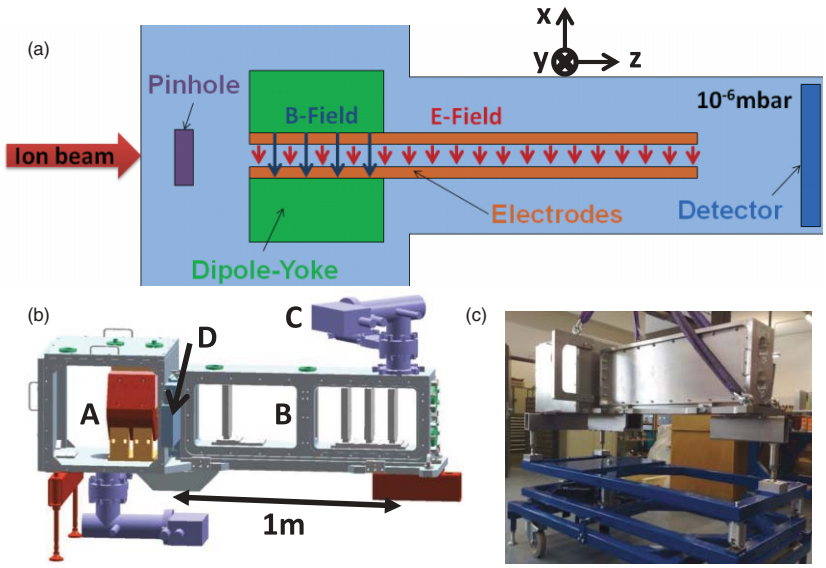

FIG. 1. (Color online) (a) Sketch of a standard TP, where the parallel magnetic and electric fields are perpendicular to the ion propagation direction. Ions are detected at the detector plane on parabolically shaped lines. (b) Schematics of the new TP with (A) the core part containing the magnets and electrodes and (B) the drift and detector part and space for an additional pair of electrodes. Both parts are separated by a vacuum valve (D) and pumped by their own cryo pump (C). (c) Photograph of the new TP, including its six-axis support.

II. THEORY

A TP ion analyzer consists of a homogeneous magnetic and electric field, where the electric field is parallel to the magnetic field and both fields are perpendicular to the ion propagation direction [see Fig. 1(a)]. In laser ion acceleration experiments, the field strengths are typically on the order of a few hundred mT for the magnetic field and several kV/cm for the electric field. The equations of motion for ions passing the TP can be calculated by the Lorentz force, which in mks units is

$$\frac{d\vec{p}}{dt} = q\left(\vec{E} + \frac{\vec{p}}{m\gamma} \times \vec{B}\right), \tag{1}$$

where m, q, $\vec{E}$, and $\vec{B}$ are the ion mass, charge, the electric field, and the magnetic field, respectively, and $\vec{p}$ the relativistic momentum and γ the Lorentz factor; time is measured in the laboratory frame. Taking into account the ion's flight (drift) after exiting the fields, one can calculate the ion traces on the detector plane perpendicular to the ion's propagation direction as a function of their initial kinetic energy and their charge to mass ratio. In the nonrelativistic case, a first order Taylor expansion yields the well-known parabola equation

$$y^2 = \frac{qB^2 l_B^2 \left(D_B + 0.5 l_B\right)^2}{m E l_E \left(D_E + 0.5 l_E\right)} x\,, \tag{2}$$

where x and y describe the ion deflection in the plane perpendicular to the ion propagation direction resulting from an E- and B-field of length l_E and l_B and after a drift length D_B and D_E measured from the end of the magnetic and electric field, respectively. Since this formula only holds for nonrelativistic energies, all calculations presented here are based on the relativistic Lorentz equation solved with a standard fourth order Runge–Kutta algorithm,[22] assuming constant E and B fields with no fringe fields.

The main factors contributing to the intrinsic resolution of a TP for a specific charge to mass ratio are the drift length and the pinhole size used to limit and collimate the incoming ion beam and the properties of the magnetic field, i.e., its strength and length along the ion propagation direction. While a longer and stronger magnetic field increases energy resolution by higher dispersion, a larger pinhole decreases resolution due to an increased ion beam spot size on the detector. Although decreasing the pinhole diameter and increasing the drift will improve contrast of a TP, both methods will decrease the ion flux on the detector. Hence, an increase in magnetic field parameters is favorable. The intrinsic instrument resolution $\Delta E_{kin}/E_{kin}$ can be approximated in the nonrelativistic case via the parabola equation [Eq. (2)] by calculating the energy range covered by the beam spot on the detector divided by its center energy

$$\frac{\Delta E_{kin}}{E_{kin}} = \frac{2s}{y\left(1 - \left(\frac{s}{2y}\right)^2\right)^2} \approx \frac{2s}{y}\,, \tag{3}$$

where y is $\left(qBl_B\left(D_B + 0.5 l_B\right)/(2mE_{kin})^{0.5}\right.$ and s the ion beam spot size on the detector given by the pinhole size and the distances between the ion source, the pinhole, and the detector plane.

On the other side, separation of different charge to mass ratios depends on the electric field parameters and the drift together with the beam spot size on the detector. The "merging" energy of two neighboring traces is calculated by the intersection point of the upper and lower boundary of the respective parabola traces, where the boundaries are given by the beam spot size on the detector. From the classic parabola equation [Eq. (2)], i.e., in the nonrelativistic limit, one can approximate

the merging energy E_{m} for a pair of two different ion species as

$$E_m = \frac{q_i E l_{\mathrm{E}} (D_{\mathrm{E}} + 0.5 l_{\mathrm{E}})}{s R_{\mathrm{Q}}}, \tag{4}$$

where $R_Q = (Q_1 + Q_2)/(Q_1 - Q_2)$ with $Q_1 = q_1/m_1 > Q_2$ and E_{m} denotes the merging energy of the ion species having the charge q_i.

III. SPECTROMETER DESIGN AND BENCHMARKING

From Eqs. (3) and (4), it is obvious that the magnetic and electric field parameters have to be increased in order to obtain extremely high energy resolution and separation of traces. The TP, we designed, consists of two vacuum compartments separated by a vacuum valve, where the first part forms the core of the TP with two 20 cm long NdFeB magnets with a 4 cm gap. The magnets are surrounded by a heavy yoke structure so that a field of 0.91 T expands almost uniformly over the whole 20 cm with a very sharp drop off at the edges. Within the magnets, a pair of copper electrodes is separated by 2 cm (parallel); we here chose a parallel design instead of a wedged one, as proposed in Ref. 23, to favor an extremely high potential of 40 kV (±20 kV each side) without vacuum breakdown.[24] In the second part of the TP—predominantly used as drift and detector area—another pair of electrodes with a length of 30 cm and variable separation (wedged or parallel) can be added to further increase separation of traces in exchange for an increased low energy cut-off. Using both electrodes at full potential (±20 kV) and 2 cm spacing (parallel) protons and C^{6+} ions will collide with the electrodes below energies of 8 MeV and 4 MeV/nucleon, respectively. To eliminate vacuum breakdown (sparking) of the electrodes due to residual gas, a pressure of $\sim 10^{-7}$ mbar is achieved by cryo pumps attached to each of the two TP parts; with this system, a pump-down time of less than 5 min between shots is achieved. The second part of the TP offers a drift region of 0.3 up to 1 m and space for different detector systems [see Fig. 1(b)]. Fused silica windows enable use of a wide range of online detectors such as a scintillator[25] or a MCP (Ref. 26). CR39 nuclear track detectors[27] or image plates (IPs) (Ref. 28) can also be used, where the two-body design of this TP allows for individual venting to change detectors within minutes without sacrificing vacuum in the core area. The TP is easily aligned with a six-axis microscale support, specifically designed and built to carry the entire TP structure. In Fig. 2, we compare the TP energy resolution for carbon C^{6+} using a drift of 0.5 m [1 m] and a 200 μm pinhole with two other TPs; the first one is the predecessor of the new TP presented here, which have both been used in Ref. 18 (hereafter referenced as "TP-H" with 0.57 T over 100 and 478 mm drift) and the TP described in Ref. 23 (hereafter referenced as "TP-C" with 0.6 T over 50 and 195 mm drift), both reflecting commonly used TP parameters for measuring ions from laser ion acceleration. Aiming for an energy resolution of better than 10% the TP-C only gives a feasible resolution at very low energies below 10 MeV/nucleon and the TP-H has reached its useability at 100 MeV/nucleon, while

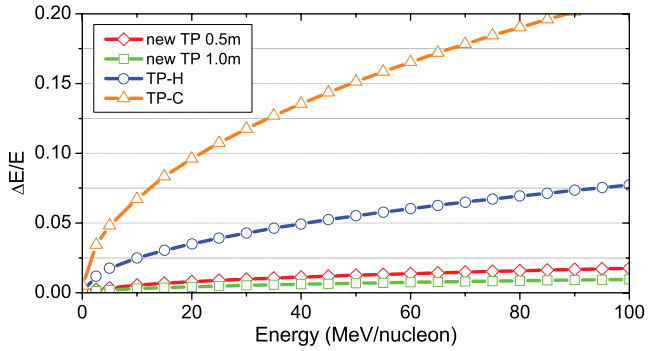

FIG. 2. (Color online) Comparison of TP resolution for carbon C^{6+} ions: new high resolution TP (red diamonds, [green squares]) with 0.91 T over 20 and 50 cm [100 cm] drift, TP-H used in Ref. 18 (blue circles) with 0.57 T over 10 and 47.8 cm drift, TP-C described in Ref. 23 (orange triangles) with 0.6 T over 5 and 19.5 cm drift. All calculations are done with a 200 μm pinhole 1 m behind the ion source.

the new TP still gives a superior resolution below 5% at these energies.

Table I compares merging energies of our new TP with a drift of 0.5 m [1 m] and a 200 μm pinhole with the two aforementioned TPs, where TP-C uses a 6 kV potential over 20 cm in a wedged configuration and TP-H uses a pair of parallel electrodes with 15 kV/2 cm over 40 cm. From Table I, it is clear that only the new TP presented here has reasonable high merging energies far above 50 MeV/nucleon. To our knowledge, no TP currently used in laser ion acceleration has enough resolution to effectively measure ions in the new acceleration regimes such as BOA and RPA when the ion energies surpass 50 MeV/nucleon. Note that the main issue is not the insufficient energy resolution but rather a too low dispersion between different species resulting in merging energies that will render distinction of different ion species and their high energy cut-off impossible.

The new high resolution and high separation TP has been benchmarked at the Los Alamos National Laboratory TRIDENT laser system using ions accelerated in the BOA regime with a 80 J and 550 fs pulse at a wavelength of 1054 nm (160 TW). The laser is focused using an F/3 off axis parabolic mirror to a spot of 6 μm (first airy minimum) resulting in an intensity of $> 2 \times 10^{20}$ W/cm^2. For the benchmarking of the TP ultrathin freestanding diamond like carbon foils of 100 nm thickness are illuminated at normal incidence to provide a beam of protons and carbon C^{4+} to C^{6+} ions of up to 67 MeV and 40 MeV/nucleon, respectively. Here, the

TABLE I. Comparison of calculated merging energies of C^{6+} into C^{5+} and C^{6+} into H^+ and vice versa in MeV/nucleon using a 200 μm pinhole placed 1 m behind the ion source; values are shown for the new TP (TP-0.5 with 0.5 m and TP-1 with 1 m drift, two pairs of electrodes (40 kV/2 cm) and TP-H (Ref. 18) and TP-C (Ref. 23) (see text for details).

	TP-C	TP-H	New TP-0.5	New TP-1
C^{5+} into C^{6+}	~3.3	13	25	59
C^{6+} into C^{5+}	~4.8	19	36	84
C^{6+} into H^+	~11.6	44	78	165
H^+ into C^{6+}	~46	164	282	553

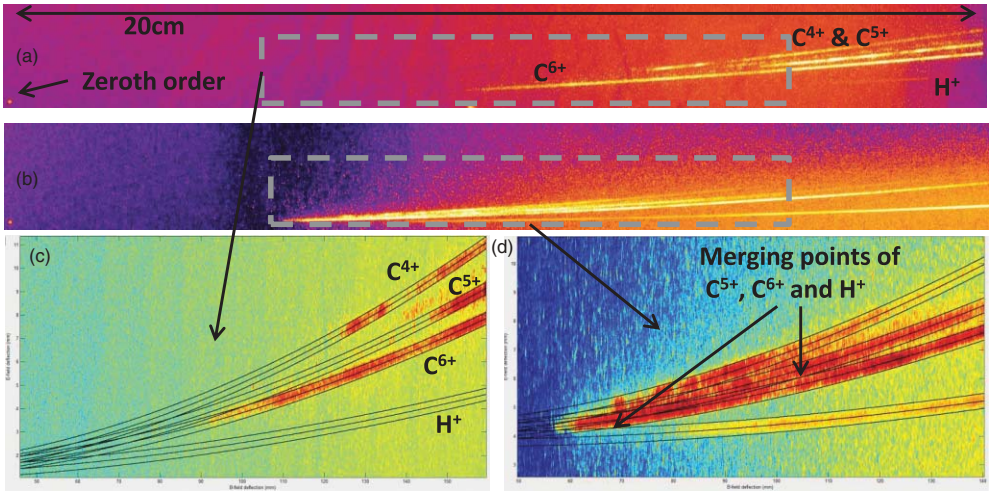

FIG. 3. (Color online) Comparison of ion spectra with identical high energy cut-off for C^{6+} (280 MeV) and C^{5+} (120 MeV) obtained using the novel high resolution and high separation TP with different drift and electric field to demonstrate influence on merging of traces: (a) spectrum obtained using appropriate parameters (25 kV/2 cm over 20 and 50 cm drift) to resolve different traces as shown in (c); (b) spectrum obtained with too low dispersion (15 kV/2 cm over 20 and 30 cm drift) resulting in premature merging of traces as shown in (d); low to high energy from right to left side of each image, black lines in (c) and (d) are predicted traces with upper and lower boundaries.

TP's drift length and electric field have been adjusted to lower values to fit the ion beam and show the influence of those parameters on the quality of the measured ion spectra.

In Fig. 3, we show two exemplary ion spectra recorded on IPs having an identical high energy cut-off for C^{5+} and C^{6+} of 80 and 280 MeV, respectively. The spectrum in Fig. 3(a) was taken using appropriate field parameters and drift length for these ion energies (25 kV/2 cm over 20 cm and 0.5 m drift); the spectrum in Fig. 3(b) was obtained with values too low for these energies (15 kV/2 cm over 20 cm and 0.3 m drift), but still exceeding those commonly used for TPs in laser ion acceleration. The ion spectra have been analyzed using software we developed to quickly analyze TP traces in terms of ion species, their energy, merging points, and resolution. Here, IPs were used as detector and ordinate values are hence given in photo stimulated luminescence (PSL) (see Ref. 28) as an IP calibration for carbon ions is not published yet. In general, measurement of absolute particle numbers is possible by this TP depending on the detector (e.g., CR39) and/or the availability of an absolute detector calibration. While the spectrum obtained with appropriate parameters shows excellent separation [see Figs. 3(a) and 3(c)], the spectrum obtained with only 15 kV/2 cm and a drift of 30 cm shows severe merging of traces [see Figs. 3(b) and 3(d)]. This renders a correct analysis above the merging point almost impossible, i.e., the extracted energy spectra of single traces will be corrupted by their neighboring species and unambiguous extraction of the cut-off energy will be difficult or even impossible; especially in experimental investigation of ion acceleration mechanisms such as RPA, analysis often relies on the high energy tail of the spectrum and could lead to false interpretation. Figure 4 shows the C^{6+} spectrum extracted from Fig. 3(b) where one can see significant corruption of the spectral shape arising from the merging of C^{5+} into C^{6+} at energies E_m [see Eq. (4)] of ~50 MeV (4.2 MeV/nucleon) and ~80 MeV (6.7 MeV/nucleon), respectively.

While these first results demonstrate the superior resolution of our new TP compared to other instruments currently in use, they do not yet exploit its full capabilities. In particular, theoretical studies predict extreme ion energies up to 400 MeV/nucleon with laser parameters that will become available in the near future.[29] To demonstrate that our TP will also yield good resolution under such conditions, Fig. 5 shows a simulated detector image as it would be measured by our new TP at a maximum electric field of 40 kV/2 cm over 50 cm and a drift of 1 m assuming high energy cut-offs for C^{6+} and H^+, as given in Ref. 29 of ~400 MeV/nucleon and 500 MeV, respectively; the energy resolution $\Delta E/E$ for proton and carbon ions at these energies is still better than 10% in our TP. Here, no merging of the C^{6+} and H^+ traces occurs, as the H^+ cut-off energy is still below the merging energy of the new TP using optimal parameters (see Table I), allowing clean extraction of the energy spectra and cut-off energies even in the extreme case studied in Ref. 29. Our detector therefore does not only provide the necessary capabilities to study current

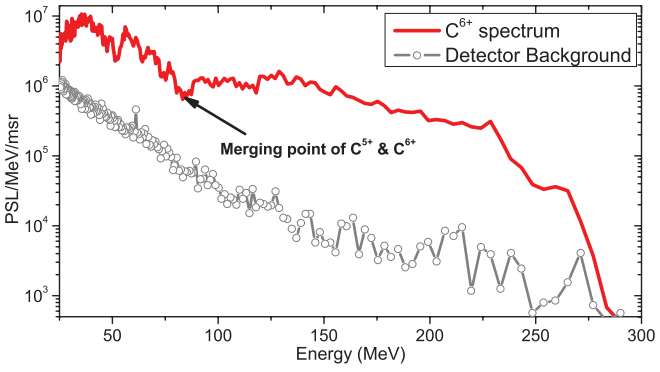

FIG. 4. (Color online) Carbon C^{6+} spectrum (red solid line) extracted from Fig. 3(b) including detector background (gray with circles) showing corruption of the spectrum after the merging of C^{5+} into C^{6+} at 80 MeV.

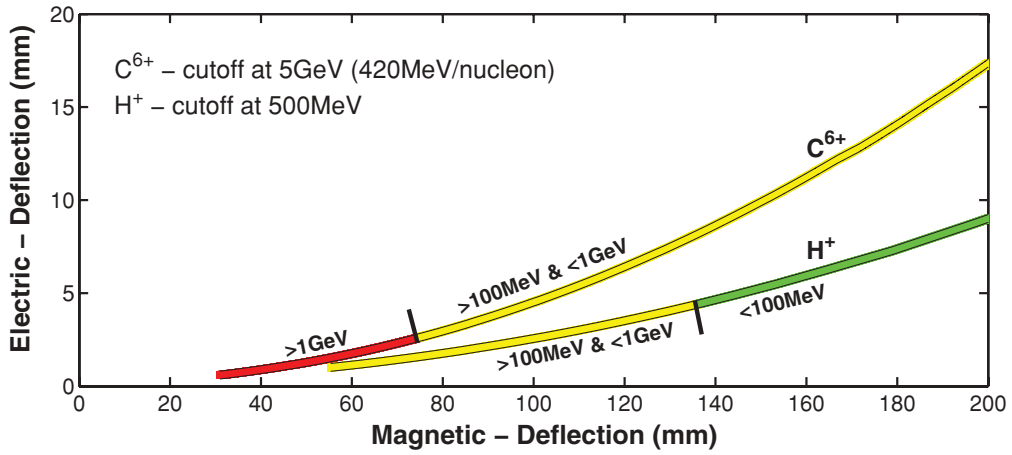

FIG. 5. (Color online) Simulated detector image showing C^{6+} and H^+ with cut-off energies of 420 MeV/nucleon and 500 MeV, respectively, as published in Ref. 29. Merging of C^{6+} into H^+ would occur at energies of 145 MeV/nucleon and 553 MeV, respectively (see Table I). Color coding: red part above 1 GeV, yellow 100 MeV to 1 GeV, and green below 100 MeV total kinetic energy.

state-of-the-art ion sources with high resolution, but will also be able to do so in experiments envisioned for the future.

IV. CONCLUSIONS

The advent of novel laser ion acceleration schemes such as BOA and RPA is followed by a tremendous energy increase of laser accelerated ions. Due to the nature of laser ion acceleration, one has to deal with a mixture of several ion species at energies eventually exceeding 100 MeV/nucleon. Current ion spectrometers are not suitable to accurately analyze such ion beams owing to their limited energy resolution and their incapability to separate traces of different ion species. In this paper, we presented a comprehensive analysis of resolution and trace separation that led to the construction of a new TP to measure such high energy ion beams with excellent energy resolution and without suffering from premature merging of ion traces. We showed experiment and simulated data demonstrating the superior capabilities of our new diagnostic at energies exceeding 100 MeV/nucleon. Our new instrument allows, for the first time, high precision measurements of laser accelerated ions in this energy range and therefore allows us to explore novel acceleration regimes such as RPA and BOA.

ACKNOWLEDGMENTS

We acknowledge expert support of the machine shop of the University of Munich in building this Thomson Parabola.

[1]M. Hegelich, S. Karsch, G. Pretzler, D. Habs, K. Witte, W. Guenther, M. Allen, A. Blazevic, J. Fuchs, J. C. Gauthier, M. Geissel, P. Audebert, T. Cowan, and M. Roth, Phys. Rev. Lett. **89**, 085002 (2002).
[2]T. E. Cowan, J. Fuchs, H. Ruhl, A. Kemp, P. Audebert, M. Roth, R. Stephens, I. Barton, A. Blazevic, E. Brambrink, J. Cobble, J. Fernández, J.-C. Gauthier, M. Geissel, M. Hegelich, J. Kaae, S. Karsch, G. P. Le Sage, S. Letzring, M. Manclossi, S. Meyroneinc, A. Newkirk, H. Pépin, and N. Renard-LeGalloudec, Phys. Rev. Lett. **92**, 204801 (2004).
[3]A. Henig, D. Kiefer, K. Markey, D. C. Gautier, K. A. Flippo, S. Letzring, R. P. Johnson, T. Shimada, L. Yin, B. J. Albright, K. J. Bowers, J. C. Fernández, S. G. Rykovanov, H.-C. Wu, M. Zepf, D. Jung, V. K. Liechtenstein, J. Schreiber, D. Habs, and B. M. Hegelich, Phys. Rev. Lett. **103**, 045002 (2009).
[4]T. Tajima, D. Habs, and X. Yan, Rev. Accel. Sci. Technol. **2**, 201 (2009).
[5]A. J. Mackinnon, P. K. Patel, M. Borghesi, R. C. Clarke, R. R. Freeman, H. Habara, S. P. Hatchett, D. Hey, D. G. Hicks, S. Kar, M. H. Key, J. A. King, K. Lancaster, D. Neely, A. Nikkro, P. A. Norreys, M. M. Notley, T. W. Phillips, L. Romagnani, R. A. Snavely, R. B. Stephens, and R. P. J. Town, Phys. Rev. Lett. **97**, 045001 (2006).
[6]M. Roth, T. E. Cowan, M. H. Key, S. P. Hatchett, C. Brown, W. Fountain, J. Johnson, D. M. Pennington, R. A. Snavely, S. C. Wilks, K. Yasuike, H. Ruhl, F. Pegoraro, S. V. Bulanov, E. M. Campbell, M. D. Perry, and H. Powell, Phys. Rev. Lett. **86**, 436 (2001).
[7]J. C. Fernández, B. J. Albright, K. A. Flippo, B. M. Hegelich, T. J. Kwan, M. J. Schmitt, and L. Yin, J. Phys.: Conf. Ser. **112**, 022051 (2008).
[8]S. P. Hatchett, C. G. Brown, T. E. Cowan, E. A. Henry, J. S. Johnson, M. H. Key, J. A. Koch, A. B. Langdon, B. F. Lasinski, R. W. Lee, A. J. Mackinnon, D. M. Pennington, M. D. Perry, T. W. Phillips, M. Roth, T. C. Sangster, M. S. Singh, R. A. Snavely, M. A. Stoyer, S. C. Wilks, and K. Yasuike, Phys. Plasmas **7**, 2076 (2000).
[9]R. A. Snavely, M. H. Key, S. P. Hatchett, T. E. Cowan, M. Roth, T. W. Phillips, M. A. Stoyer, E. A. Henry, T. C. Sangster, M. S. Singh, S. C. Wilks, A. MacKinnon, A. Offenberger, D. M. Pennington, K. Yasuike, A. B. Langdon, B. F. Lasinski, J. Johnson, M. D. Perry, and E. M. Campbell, Phys. Rev. Lett. **85**, 2945 (2000).
[10]B. M. Hegelich, B. Albright, P. Audebert, A. Blazevic, E. Brambrink, J. Cobble, T. Cowan, J. Fuchs, J. C. Gauthier, C. Gautier, M. Geissel, D. Habs, R. Johnson, S. Karsch, A. Kemp, S. Letzring, M. Roth, U. Schramm, J. Schreiber, K. J. Witte, and J. C. Fernandez, Phys. Plasmas **12**, 56314 (2005).
[11]O. Klimo, J. Psikal, J. Limpouch, and V. T. Tikhonchuk, Phys. Rev. ST Accel. Beams **11**, 031301 (2008).
[12]X. Q. Yan, C. Lin, Z. M. Sheng, Z. Y. Guo, B. C. Liu, Y. R. Lu, J. X. Fang, and J. E. Chen, Phys. Rev. Lett. **100**, 135003 (2008).
[13]A. Henig, S. Steinke, M. Schnürer, T. Sokollik, R. Hörlein, D. Kiefer, D. Jung, J. Schreiber, B. M. Hegelich, X. Q. Yan, J. Meyer-ter Vehn, T. Tajima, P. V. Nickles, W. Sandner, and D. Habs, Phys. Rev. Lett. **103**, 245003 (2009).
[14]T. Esirkepov, M. Borghesi, S. V. Bulanov, G. Mourou, and T. Tajima, Phys. Rev. Lett. **92**, 175003 (2004).
[15]L. Yin, B. J. Albright, B. M. Hegelich, K. J. Bowers, K. A. Flippo, T. J. T. Kwan, and J. C. Fernandez, Phys. Plasmas **14**, 56706 (2007).
[16]B. J. Albright, L. Yin, K. J. Bowers, B. M. Hegelich, K. A. Flippo, T. J. T. Kwan, and J. C. Fernandez, Phys. Plasmas **14**, 94502 (2007).
[17]A. Macchi, S. Veghini, and F. Pegoraro, Phys. Rev. Lett. **103**, 085003 (2009).
[18]B. M. Hegelich, L. Yin, B. J. Albright, K. Bowers, K. Flippo, D. C. Gautier, A. Henig, R. Hörlein, R. Johnson, D. Jung, D. Kiefer, S. Letzring, R. Shah, T. Shimada, T. Tajima, X. Yan, D. Habs, and J. C. Fernández, private communication.

[19]J. J. Thomson, Philos. Mag. Ser. **22**, 469 (1911).
[20]J. Workman, J. Cobble, K. Flippo, D. C. Gautier, and S. Letzring, Rev. Sci. Instrum. **79**, 10E905 (2008).
[21]R. C. Shah, R. P. Johnson, T. Shimada, K. A. Flippo, J. C. Fernandez, and B. M. Hegelich, Opt. Lett. **34**, 2273 (2009).
[22]M. Abramowitz and I. A. Stegun, *Handbook of Mathematical Functions Applied Mathematics Series*, Volume 55 (Washington: National Bureau of Standards; reprinted 1968 by Dover Publications, New York) Paragraph 25.5.
[23]D. Carroll, P. Brummitt, D. Neely, F. Lindau, O. Lundh, C.-G. Wahlström, and P. McKenna, Nucl. Instrum. Methods Phys. Res. A **620**, 23 (2010).
[24]F. Paschen, Ann. Phys. **273**, 69 (1889).
[25]A. P. L. Robinson, P. Foster, D. Adams, D. C. Carroll, B. Dromey, S. Hawkes, S. Kar, Y. T. Li, K. Markey, P. McKenna, C. Spindloe, M. Streeter, C.-G. Wahlström, M. H. Xu, M. Zepf, and D. Neely, New J. Phys. **11**, 083018 (2009).
[26]K. Harres, M. Schollmeier, E. Brambrink, P. Audebert, A. Blazevic, K. Flippo, D. C. Gautier, M. Geissel, B. M. Hegelich, F. Nurnberg, J. Schreiber, H. Wahl, and M. Roth, Rev. Sci. Instrum. **79**, 93306 (2008).
[27]R. L. Fleischer, P. B. Price, and R. M. Walker, J. Appl. Phys. **36**, 3645 (1965).
[28]I. J. Paterson, R. J. Clarke, N. C. Woolsey, and G. Gregori, Meas. Sci. Technol. **19**, 095301 (2008).
[29]T.-P. Yu, A. Pukhov, G. Shvets, and M. Chen, Phys. Rev. Lett. **105**, 065002 (2010).